PCCP

ROYAL SOCIETY OF CHEMISTRY

ARTICLE TYPE

Cite this: DOI: 10.1039/xxxxxxxxxx

Nonrelativistic energy levels of HD

Krzysztof Pachucki,[a] and Jacek Komasa[b]

Received Date
Accepted Date

DOI: 10.1039/xxxxxxxxxx

www.rsc.org/journalname

Nonadiabatic exponential functions are employed to solve the four-body Schrödinger equation. Nonrelativistic bound energy levels of the HD molecule are calculated to the relative accuracy of $10^{-12}-10^{-13}$, which is the first step toward highly accurate prediction of dissociation and transition energies. Such energies, in connection with equally accurate experimental data, will enable refinement of the physical constant and aid the search for deviations caused by yet unknown interactions at the atomic scale.

1 Introduction

For the hydrogen molecule and its isotopic variants, contemporary spectroscopic measurements have reached the accuracy of 10^{-5}-$10^{-6}\,\mathrm{cm}^{-1}$ for selected transition energies.[1–7] However, different experiments do not always agree within the claimed accuracy. In particular, for the $R(1)$ transition in the $(2,0)$ overtone band in HD, Cozijn et al.[5] have determined this transition energy to the accuracy of $7\cdot10^{-7}\,\mathrm{cm}^{-1}$ (20 kHz), whereas Tao et al.[7] have reached the accuracy of $3\cdot10^{-6}\,\mathrm{cm}^{-1}$ (80 kHz) with results that differ among themselves by about $3\cdot10^{-5}\,\mathrm{cm}^{-1}$ (900 kHz). Theoretical calculations could resolve this discrepancy provided a sufficient accuracy (of ca. $10^{-5}\,\mathrm{cm}^{-1}$) is achieved. This requires calculations of nonadiabatic corrections to the quantum electrodynamic contribution, which will be feasible in the near future.

The accuracy of theoretical predictions is ultimately limited by uncertainties in the nucleus-electron mass ratios. For example, the difference between the CODATA 2014 proton-electron mass ratio ($\mu_\mathrm{p}=m_\mathrm{p}/m_\mathrm{e}$) and the value reported most recently[8] leads to a difference of about $7\cdot10^{-7}\,\mathrm{cm}^{-1}$ (20 kHz) for the $R(1)$ transition. This means that sufficiently accurate calculations of higher-order quantum electrodynamical effects may lead to the improved determination of the proton-electron mass ratio. Eventually, if one observes any discrepancies that can not be accommodated by physical constants, it will indicate the presence of yet unknown interaction that goes beyond the Standard Model.

On the theoretical side, various relativistic and quantum electrodynamic corrections have recently been calculated to a high accuracy,[9,10] but the principal problem up to now has been the insufficient accuracy of nonrelativistic energy levels. The purpose of this work is to present a method which enables the uncertainty originating from the nonrelativistic energy to be practically removed from the overall energy budget. This method aims at the precision level of $10^{-7}\,\mathrm{cm}^{-1}$ for the dissociation energy of an arbitrary rovibrational energy level.

From a historical point of view, our work is related to the classic paper by Kołos and Wolniewicz.[11] Although, our formalism differs significantly from the one used in their work, that article deserves a mention as the first attempt of a fully nonadiabatic description of the hydrogen molecule. Later on, the nonadiabatic corrections for rovibrational levels were evaluated in frames of the adiabatic approximation by Wolniewicz[12] in 1995 and by us[13] in 2010. Two lowest nonrotational levels were studied within a nonadiabatic formalism by Stanke et al.[14] in 2009.

2 Theory

Our aim is to find highly accurate variational solutions to the stationary Schrödinger equation $\hat{H}\Psi=E\Psi$ for a heteronuclear diatomic molecule with the nuclei of charge Z_A and Z_B and finite masses M_A and M_B. The four-body Coulomb Hamiltonian for such a system, in atomic units and with a common notation, reads

$$\hat{H}=-\frac{1}{2M_A}\nabla_A^2-\frac{1}{2M_B}\nabla_B^2-\frac{1}{2m_\mathrm{e}}\nabla_1^2-\frac{1}{2m_\mathrm{e}}\nabla_2^2 + \frac{Z_AZ_B}{r_{AB}}+\frac{1}{r_{12}}-\frac{Z_A}{r_{1A}}-\frac{Z_A}{r_{2A}}-\frac{Z_B}{r_{1B}}-\frac{Z_B}{r_{2B}}\,. \tag{1}$$

We search for both the eigenvalues E representing energy of bound rovibrational levels and the eigenfunctions Ψ which will be employed in future studies of relativistic and electrodynamic energy corrections.

A properly constructed trial wave function must reflect all symmetries and angular momenta present in the molecule. We assume that the rotational angular momentum of nuclei couples to the electronic angular momentum, $\vec{L}$, to form the total angular momentum $\vec{J}$ of the molecule. Therefore, for a given rotational level J the wave function $\Psi^{J,M}$, which formally depends also on M—the projection of $\vec{J}$ on the Z-axis in the laboratory frame, must

[a] Faculty of Physics, University of Warsaw, Pasteura 5, 02-093 Warsaw, Poland. E-mail: krp@fuw.edu.pl
[b] Faculty of Chemistry, Adam Mickiewicz University, Umultowska 89b, 61-614 Poznań, Poland. E-mail: komasa@man.poznan.pl

involve ingredients describing the subsequent electronic states. The quantum number Λ—the eigenvalue of the $\vec{n}\cdot\vec{L}$ operator and the inversion symmetry symbol g or u (for gerade or ungerade) are employed to distinguish between such states: $\Sigma_{g,u}$, $\Pi_{g,u}$, $\Delta_{g,u}$, ... Our Ansatz is a sum of components with growing Λ

$$\Psi^{J,M} = \Psi^{J,M}_{\Sigma_g} + \Psi^{J,M}_{\Sigma_u} + \Psi^{J,M}_{\Pi_g} + \Psi^{J,M}_{\Pi_u} + \Psi^{J,M}_{\Delta_g} + \Psi^{J,M}_{\Delta_u} + \dots \qquad (2)$$

where

$$\Psi^{J,M}_{\Sigma_{g,u}} = Y^J_M \, \Phi^J_{\Sigma_{g,u}}, \qquad \text{for } J \geq 0 \qquad (3)$$

$$\Psi^{J,M}_{\Pi_{g,u}} = \sqrt{\frac{2}{J(J+1)}} R \rho^i \left(\nabla^i_R Y^J_M\right) \Phi^J_{\Pi_{g,u}}, \qquad \text{for } J \geq 1 \qquad (4)$$

$$\Psi^{J,M}_{\Delta_{g,u}} = \sqrt{\frac{4}{(J-1)J(J+1)(J+2)}} R^2 \, (\rho^i \rho'^j)^{(2)} \times \left(\nabla^i_R \nabla^j_R Y^J_M\right) \Phi^J_{\Delta_{g,u}}, \qquad \text{for } J \geq 2 \qquad (5)$$

and so on for the higher electronic angular momenta. In the above equations we use the following notation

$$(\rho^i \rho'^j)^{(2)} \equiv \frac{1}{2}\left(\rho^i \rho'^j + \rho^j \rho'^i - \left(\delta^{ij} - n^i n^j\right) \vec{\rho}\cdot\vec{\rho}\,'\right), \qquad (6)$$

where $\vec{\rho}, \vec{\rho}\,' \equiv \vec{\rho}_1$ or $\vec{\rho}_2$, $n^i \equiv R^i/R$ and $\rho^i_a = \left(\delta^{ij} - n^i n^j\right) r^j_{aB}$, with the Einstein summation convention assumed. The $Y^J_M = Y^J_M(\vec{n})$ denotes a spherical harmonic. The functions Φ^J_Λ represent linear expansions

$$\Phi^J_\Lambda = R^J \sum_{\{k\}} c_{\{k\}} \left(1 + \mathscr{P}_{12}\right) \Phi^J_{\Lambda\{k\}} \qquad (7)$$

in the following nonadiabatic James-Coolidge (naJC) basis functions

$$\Phi_{\{k\}} = e^{-\alpha R - \beta(\zeta_1+\zeta_2)} R^{k_0} r_{12}^{k_1} \eta_1^{k_2} \eta_2^{k_3} \zeta_1^{k_4} \zeta_2^{k_5} \qquad (8)$$

with $\zeta_1 = r_{1A} + r_{1B}$, $\eta_1 = r_{1A} - r_{1B}$, $\zeta_2 = r_{2A} + r_{2B}$, $\eta_2 = r_{2A} - r_{2B}$, and $\vec{R} = \vec{r}_{AB}$. The α and β denote nonlinear variational parameters and k_i are non-negative integers collectively denoted as $\{k\}$. The basis functions with $k_2 + k_3$ even (odd) have the subscript g (u).

The trial four-particle wave function defined above depends explicitly on interparticle distances only, i.e. it is translationally invariant and our results do not depend on the choice of the origin in space.

Evaluation of the overlap and Hamiltonian matrix elements in the naJC basis $\Phi_{\{k\}}$ was described in detail elsewere[15] and will not be repeated here.

Due to the mutual orthogonality of the basis functions belonging to different electronic symmetries ($\langle\Phi_\Lambda|\Phi_{\Lambda'}\rangle = \delta^{\Lambda'\Lambda}$), the overlap matrix $\mathbb{N}$ has a block-diagonal structure whereas the Hamiltonian matrix $\mathbb{H}$ is block-band diagonal because $\langle\Phi_\Lambda|\hat{H}|\Phi_{\Lambda'}\rangle = 0$ whenever $|\Lambda - \Lambda'| > 1$, see Eqs. (9) and (10).

$$\mathbb{N} = \begin{pmatrix} \mathbb{N}_{\Sigma_g\Sigma_g} & 0 & 0 & 0 & 0 & 0 & \cdots \\ 0 & \mathbb{N}_{\Sigma_u\Sigma_u} & 0 & 0 & 0 & 0 & \cdots \\ 0 & 0 & \mathbb{N}_{\Pi_g\Pi_g} & 0 & 0 & 0 & \cdots \\ 0 & 0 & 0 & \mathbb{N}_{\Pi_u\Pi_u} & 0 & 0 & \cdots \\ 0 & 0 & 0 & 0 & \mathbb{N}_{\Delta_g\Delta_g} & 0 & \cdots \\ 0 & 0 & 0 & 0 & 0 & \mathbb{N}_{\Delta_u\Delta_u} & \cdots \\ \vdots & \vdots & \vdots & \vdots & \vdots & \vdots & \ddots \end{pmatrix} \qquad (9)$$

$$\mathbb{H} = \begin{pmatrix} \mathbb{H}_{\Sigma_g\Sigma_g} & \mathbb{H}_{\Sigma_g\Sigma_u} & \mathbb{H}_{\Sigma_g\Pi_g} & \mathbb{H}_{\Sigma_g\Pi_u} & 0 & 0 & \cdots \\ \mathbb{H}_{\Sigma_u\Sigma_g} & \mathbb{H}_{\Sigma_u\Sigma_u} & \mathbb{H}_{\Sigma_u\Pi_g} & \mathbb{H}_{\Sigma_u\Pi_u} & 0 & 0 & \cdots \\ \mathbb{H}_{\Pi_g\Sigma_g} & \mathbb{H}_{\Pi_g\Sigma_u} & \mathbb{H}_{\Pi_g\Pi_g} & \mathbb{H}_{\Pi_g\Pi_u} & \mathbb{H}_{\Pi_g\Delta_g} & \mathbb{H}_{\Pi_g\Delta_u} & \cdots \\ \mathbb{H}_{\Pi_u\Sigma_g} & \mathbb{H}_{\Pi_u\Sigma_u} & \mathbb{H}_{\Pi_u\Pi_g} & \mathbb{H}_{\Pi_u\Pi_u} & \mathbb{H}_{\Pi_u\Delta_g} & \mathbb{H}_{\Pi_u\Delta_u} & \cdots \\ 0 & 0 & \mathbb{H}_{\Delta_g\Pi_g} & \mathbb{H}_{\Delta_g\Pi_u} & \mathbb{H}_{\Delta_g\Delta_g} & \mathbb{H}_{\Delta_g\Delta_u} & \cdots \\ 0 & 0 & \mathbb{H}_{\Delta_u\Pi_g} & \mathbb{H}_{\Delta_u\Pi_u} & \mathbb{H}_{\Delta_u\Delta_g} & \mathbb{H}_{\Delta_u\Delta_u} & \cdots \\ \vdots & \vdots & \vdots & \vdots & \vdots & \vdots & \ddots \end{pmatrix} \qquad (10)$$

3 Solving the matrix equation

The matrix Schrödinger equation $(\mathbb{H} - E\,\mathbb{N})\,c = 0$ can be solved directly, e.g. by the inverse iteration method, or perturbatively by utilizing the fact that all off-diagonal blocks are proportional to the inverse of nuclear mass, and thus are small. The latter approach is particularly advantageous for very large basis sets—the largest expansion employed in our calculations involved 445 498 basis functions. It is based on the Rayleigh-Schrödinger perturbation expansion of the total energy

$$E = E^{(0)} + E^{(2)} + E^{(3)} + E^{(4)} + \dots \qquad (11)$$

with respect to off-diagonal blocks. The superscript n in $E^{(n)}$ corresponds to the power of the off-diagonal blocks appearing in subsequent energy corrections. The unperturbed energy $E^{(0)} = E_{\Sigma_g}$ is obtained from the 0'th order equation

$$(\mathbb{H}_{\Sigma_g\Sigma_g} - E_{\Sigma_g}\,\mathbb{N}_{\Sigma_g\Sigma_g})\,\Psi^{J,M}_{\Sigma_g} = 0 \qquad (12)$$

and is numerically several orders of magnitude larger than all the higher-order terms of the series.

The second-order term is expressed as the expectation value

$$E^{(2)} = \left\langle \Psi^{J,M}_{\Sigma_g} \middle| V(E_{\Sigma_g}) \middle| \Psi^{J,M}_{\Sigma_g} \right\rangle. \qquad (13)$$

with the perturbation operator defined by

$$V(E) = H_{\Sigma_g\Sigma_u} \frac{1}{E - H_{\Sigma_u}} H_{\Sigma_u\Sigma_g} + H_{\Sigma_g\Pi_g} \frac{1}{E - H_{\Pi_g}} H_{\Pi_g\Sigma_g} + H_{\Sigma_g\Pi_u} \frac{1}{E - H_{\Pi_u}} H_{\Pi_u\Sigma_g}. \qquad (14)$$

The third-order term reads

$$E^{(3)} = \left\langle \Psi^{J,M}_{\Sigma_g} \middle| V^{(3)} \middle| \Psi^{J,M}_{\Sigma_g} \right\rangle \qquad (15)$$

This journal is © The Royal Society of Chemistry [year]

where

$$V^{(3)} = V_{\Pi_g} \frac{1}{E_{\Sigma_g} - H_{\Pi_g}} H_{\Pi_g \Sigma_g} + V_{\Pi_u} \frac{1}{E_{\Sigma_g} - H_{\Pi_u}} H_{\Pi_u \Sigma_g} + V_{\Sigma_u} \frac{1}{E_{\Sigma_g} - H_{\Sigma_u}} H_{\Sigma_u \Sigma_g} \tag{16}$$

and involves a set of auxiliary operators appearing also in the expressions for $E^{(4)}$ below

$$V_{\Sigma_u} = H_{\Sigma_g \Pi_u} \frac{1}{E_{\Sigma_g} - H_{\Pi_u}} H_{\Pi_u \Sigma_u} + H_{\Sigma_g \Pi_g} \frac{1}{E_{\Sigma_g} - H_{\Pi_g}} H_{\Pi_g \Sigma_u} \tag{17}$$

$$V_{\Pi_g} = H_{\Sigma_g \Sigma_u} \frac{1}{E_{\Sigma_g} - H_{\Sigma_u}} H_{\Sigma_u \Pi_g} + H_{\Sigma_g \Pi_u} \frac{1}{E_{\Sigma_g} - H_{\Pi_u}} H_{\Pi_u \Pi_g} \tag{18}$$

$$V_{\Pi_u} = H_{\Sigma_g \Sigma_u} \frac{1}{E_{\Sigma_g} - H_{\Sigma_u}} H_{\Sigma_u \Pi_u} + H_{\Sigma_g \Pi_g} \frac{1}{E_{\Sigma_g} - H_{\Pi_g}} H_{\Pi_g \Pi_u} \tag{19}$$

$$V_{\Delta_g} = H_{\Sigma_g \Pi_u} \frac{1}{E_{\Sigma_g} - H_{\Pi_u}} H_{\Pi_u \Delta_g} + H_{\Sigma_g \Pi_g} \frac{1}{E_{\Sigma_g} - H_{\Pi_g}} H_{\Pi_g \Delta_g} \tag{20}$$

$$V_{\Delta_u} = H_{\Sigma_g \Pi_u} \frac{1}{E_{\Sigma_g} - H_{\Pi_u}} H_{\Pi_u \Delta_u} + H_{\Sigma_g \Pi_g} \frac{1}{E_{\Sigma_g} - H_{\Pi_g}} H_{\Pi_g \Delta_u} \tag{21}$$

The fourth-order term involves the contributions from Δ states and can be evaluated from

$$\begin{aligned} E^{(4)} = & \left\langle \Psi^{J,M}_{\Sigma_g} \middle| V(E_{\Sigma_g}) \frac{1}{(E_{\Sigma_g} - H_{\Sigma_g})'} V(E_{\Sigma_g}) \middle| \Psi^{J,M}_{\Sigma_g} \right\rangle \\ & + \left\langle \Psi^{J,M}_{\Sigma_g} \middle| \left. \frac{\partial V}{\partial E} \right|_{E_{\Sigma_g}} \middle| \Psi^{J,M}_{\Sigma_g} \right\rangle E^{(2)} + \left\langle \Psi^{J,M}_{\Sigma_g} \middle| V_{\Sigma_u} \frac{1}{E_{\Sigma_g} - H_{\Sigma_u}} V^{\dagger}_{\Sigma_u} \middle| \Psi^{J,M}_{\Sigma_g} \right\rangle \\ & + \left\langle \Psi^{J,M}_{\Sigma_g} \middle| V_{\Pi_g} \frac{1}{E_{\Sigma_g} - H_{\Pi_g}} V^{\dagger}_{\Pi_g} \middle| \Psi^{J,M}_{\Sigma_g} \right\rangle + \left\langle \Psi^{J,M}_{\Sigma_g} \middle| V_{\Pi_u} \frac{1}{E_{\Sigma_g} - H_{\Pi_u}} V^{\dagger}_{\Pi_u} \middle| \Psi^{J,M}_{\Sigma_g} \right\rangle \\ & + \left\langle \Psi^{J,M}_{\Sigma_g} \middle| V_{\Delta_g} \frac{1}{E_{\Sigma_g} - H_{\Delta_g}} V^{\dagger}_{\Delta_g} \middle| \Psi^{J,M}_{\Sigma_g} \right\rangle + \left\langle \Psi^{J,M}_{\Sigma_g} \middle| V_{\Delta_u} \frac{1}{E_{\Sigma_g} - H_{\Delta_u}} V^{\dagger}_{\Delta_u} \middle| \Psi^{J,M}_{\Sigma_g} \right\rangle . \end{aligned} \tag{22}$$

This perturbation expansion converges very rapidly, so including terms up to the fourth order appears to be sufficient to reach the desired accuracy.

4 Technical details and the convergence study

Calculations of the matrix elements as well as the linear algebra were performed in octuple-precision arithmetic.[16] Apart from a trivial matrix elements parallelization, the linear algebra tasks were also efficiently parallelized for use on both distributed and shared memory systems. In the former case we applied the Elemental library[17] in connection with MPI communication protocol, whereas in the latter—the PLASMA library[18] with OpenMP interface. The multithreading has significantly lowered the time limitations of our calculations, additionally, the distributed memory program has lifted the memory barrier.

The nonlinear parameters α and β of the basis function $\Phi_{\{k\}}$ (Eq. (8)) were determined variationally. All the basis functions have a common α exponent but separate β exponents for different Λ states. In the first step, the number of basis functions $k_i^{\max}$ saturating the energy up to the $10^{-9}\,\mathrm{cm}^{-1}$ threshold for given Λ were determined. Next, optimal α and β^{Σ_g} were found. With these two exponents fixed, the β^{Σ_u}, β^{Π_g}, and β^{Π_u} were optimized independently. The basis functions of Δ states appear in two variants necessary to make the wave function complete. One, for which $(\rho^i \rho'^j)^{(2)}$ of Eq. (6) has $\rho = \rho'$, and the other with $\rho \neq \rho'$. Both variants feature their own β^{Δ_g} and β^{Δ_u} exponents optimized in the presence of the other βs fixed.

As already mentioned, the $E^{(0)}$ contribution (see Eq. (11)) is several orders of magnitude larger than the remaining ones. For this reason, we made a special effort to converge this energy component and we employed a double basis set for its description. Such a double basis set was composed of two sets of basis functions sharing the α exponent but having their own β^{Σ_g} nonlinear parameters. The optimal parameters and the number of expansion terms were determined for both sets simultaneously.

An indispensable (and requiring serious additional effort) feature of the results of high-precision calculations is the estimated uncertainty assigned to a final result. For basis functions capable of forming a complete basis set, as it is in the present case, the uncertainty can be determined from a convergence pattern obtained by evaluation of the energy with a successively increasing expansion of the wave function. As a key parameter employed to control the energy convergence we have selected the 'shell' parameter Ω. This parameter limits the number of basis functions included in calculations to those fulfilling the inequality $\sum_{k=1}^{5} k_i \leq \Omega$, while the maximum of k_0 is fixed at the $k_0^{\max}$ value. The number of all basis functions K which meet this condition grows nonuniformly with Ω but ensures the saturation of the subsequent electronic 'shells'. The $E^{(0)}$ energy converges with growing K regularly according to the inverse power law which permits a firm extrapolation to the complete basis set and the estimation of the uncertainty. The convergence of the consecutive energy components $E^{(2)}$, $E^{(3)}$, and $E^{(4)}$ is less regular but also very rapid. As the final uncertainty changes very slowly between neighboring levels, the analysis of the convergence has been omitted for some of them. The features of the convergence are illustrated by the data collected in Table 1. The numerical convergence achieved for the individual $E^{(n)}$ terms is of the order of 10^{-13} a.u. and slowly grows with rotational or vibrational quantum number.

Another aspect of the convergence study is the saturation of these energy terms with respect to the presence of the basis functions with the growing quantum number Λ. For the nonrotational states only $\Sigma_{g,u}$ functions are required. However, with increasing J, the contributions from the Π_g and Π_u functions become more and more significant so that already for $J = 3$ their sum supersedes that from the Σ_u functions. The contribution from $\Delta_{g,u}$ functions become larger than $10^{-7}\,\mathrm{cm}^{-1}$ already for levels with $J \geq 4$, but they appear only in the fourth and higher-order terms of expansion (11). Figure 1 shows graphically how the contributions to dissociation energy from subsequent Λ states change with the growing J quantum number. The expected contribution from the $\Phi_{g,u}$ functions emerge only in terms $E^{(6)}$ and higher and may become noticeable only for the highest rotational excitations, which are not considered here. Therefore, we can safely claim that all

Table 1 Convergence of the $E^{(0)}$, $E^{(2)}$, $E^{(3)}$, and $E^{(4)}$ components (in a.u.) with the size of the basis set for the $(0,0)$ and $(0,16)$ levels. For the former level the $E^{(3)}$ vanishes

Ω	K	$E^{(0)}$	K	$E^{(2)}\cdot 10^7$	$E^{(3)}\cdot 10^9$	$E^{(4)}\cdot 10^{12}$
		$(0,0)$				
9	30 415	−1.165 471 711 202 65	31 843	−2.127 152 16		−2.233
10	45 045	−1.165 471 711 239 17	47 502	−2.127 151 84		−2.233
11	64 680	−1.165 471 711 245 14	68 712	−2.127 151 85		−2.233
12	90 860	−1.165 471 711 246 56	96 992	−2.127 151 81		−2.233
13	124 740	−1.165 471 711 246 87				
14	171 360	−1.165 471 711 246 96				
∞	∞	−1.165 471 711 246 99(3)	∞	−2.127 151 8(1)		−2.233
		$(0,16)$				
9	19 355	−1.117 302 461 466 66	70 089	−45.529 370	1.515 796	−499.944
10	28 665	−1.117 302 461 509 30	104 647	−45.529 401	1.515 800	−499.969
11	41 160	−1.117 302 461 516 85	151 524	−45.529 403	1.515 801	−499.991
12	57 820	−1.117 302 461 518 55	213 870	−45.529 406	1.515 802	−499.998
13	79 380	−1.117 302 461 518 95				
14	107 100	−1.117 302 461 519 05				
∞	∞	−1.117 302 461 519 09(3)	∞	−45.529 410(3)	1.515 802(1)	−500.01(1)

the energy levels presented in this work are saturated with respect to the electronic angular momentum.

The next question to be asked, is how large is the error in energy introduced by cutting off the series of Eq. (11) after the fourth term. Table 2 presents the individual $E^{(n)}$ contributions for a few selected states. These contributions grow polynomially with increasing J. For the $v=0, J=16$ level the $E^{(4)}$ contribution is of the order of $10^{-4}\,\mathrm{cm}^{-1}$, and it is justified to ask whether still higher-order terms are not necessary to guarantee the desired accuracy. We note that each Hamiltonian contains the $1/\mu_\mathrm{n}$ factor. Hence, we can expect that $E^{(5)}/E^{(4)} \approx 1/\mu_\mathrm{n}$ or even less, as observed in the case of the $E^{(3)}/E^{(2)}$ relation, which is approximately $-3\cdot 10^{-4}$. The above question can also be answered by a direct comparison of the energy obtained from the full matrix diagonalization with the energy evaluated using Eq. (11). Results of such computations in comparison with the simple scaling of $D^{(4)}$ by the inverse of the nuclear reduced mass are shown in Figure 2. As we can infer from this figure, the contribution from the omitted $D^{(n)}$, $n\geq 5$ terms exceeds $10^{-8}\,\mathrm{cm}^{-1}$ only for $J\geq 9$ and remains smaller than $10^{-7}\,\mathrm{cm}^{-1}$ for higher J. On the basis of the above arguments we conclude that even for the highest J considered here, the contributions from the neglected higher-order energy components are smaller than $10^{-7}\,\mathrm{cm}^{-1}$.

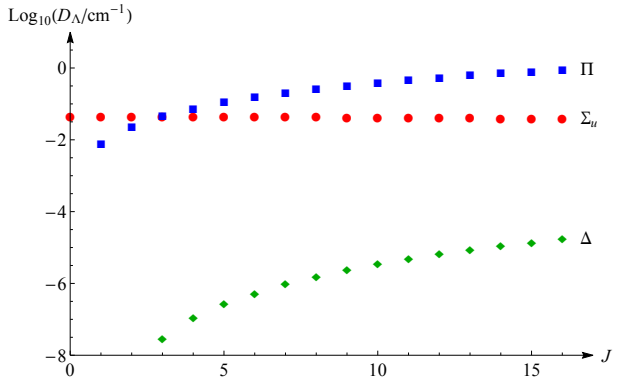

Fig. 1 The contributions from Σ_u, Π, and Δ states to the total nonrelativistic dissociation energy as a function of the rotational quantum number J (for $v=0$).

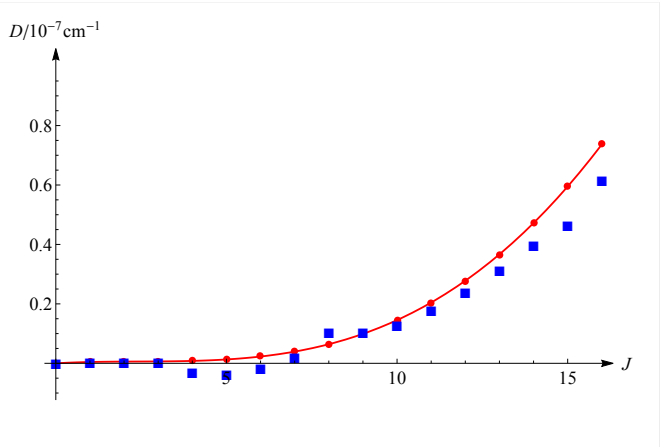

Fig. 2 The estimated contribution to the total nonrelativistic dissociation energy from the omitted $D^{(n)}$, $n\geq 5$ terms as a function of the rotational quantum number J (for $v=0$). The blue squares correspond to the computed contribution from the omitted higher order terms and the red line to the simple estimation $D^{(5)}\approx D^{(4)}/\mu_\mathrm{n}$.

5 Numerical results

Table 3 contains the final nonrelativistic energies obtained for 41 rovibrational levels, which are located up to ca. $10\,000\,\mathrm{cm}^{-1}$ above the ground level. The energy of remaining levels, obtained in frames of the nonadiabatic perturbation theory (NAPT) with the accuracy of ca. $0.0005\,\mathrm{cm}^{-1}$, is available in ref. 13. For each level, both the nonadiabatic eigenvalue $E_{v,J}$ and the correspond-

This journal is © The Royal Society of Chemistry [year]

Table 2 Convergence of the eigenvalue expansion $E = E^{(0)} + E^{(2)} + E^{(3)} + E^{(4)}$ in terms of the corresponding dissociation energy components (in cm^{-1}) for the selected levels of HD

Term	$v = 0, J = 0$	$v = 0, J = 1$	$v = 0, J = 16$	$v = 2, J = 2$
$D^{(0)}$	36406.464205 30(1)	36317.229411 80(1)	25834.535877 89(1)	29075.220383 41(1)
$D^{(2)}$	0.046685 59	0.054723 98	0.999255 03(7)	0.217588 59(2)
$D^{(3)}$	0.000000 00	−0.000002 90	−0.000332 68	−0.000009 77
$D^{(4)}$	0.000000 49	0.000000 53	0.000109 74	0.000002 98(1)
D	36406.510891 37(1)	36317.284133 42(1)	25835.534909 98(7)	29075.437965 20(3)

Table 3 Nonadiabatic eigenvalue ($E_{v,J}$) and dissociation energy ($D_{v,J}$) of the rovibrational energy levels of HD located up to ca. $10000\,\mathrm{cm}^{-1}$ above the ground level. The uncertainties assigned to $E_{v,J}$ and $D_{v,J}$ are due to the numerical convergence only and do not account for uncertainties transferred from the fundamental constants. The μ_n is the nucleus-to-electron mass ratio, with $n = p, d$

(v,J)	$E_{v,J}$/hartree	$D_{v,J}/\mathrm{cm}^{-1}$	$\frac{\partial E_{v,J}}{\partial \mu_\mathrm{p}} \cdot 10^6$	$\frac{\partial E_{v,J}}{\partial \mu_\mathrm{d}} \cdot 10^6$
(0,0)	−1.165471 923964 39(3)	36406.510891 37(1)	−1.69	−0.424
(0,1)	−1.165065 376941 65(3)	36317.284133 42(1)	−1.84	−0.459
(0,2)	−1.164255 083090 94(3)	36139.445 189 24(1)	−2.13	−0.533
(0,3)	−1.163046 575929 44(3)	35874.208 525 46(1)	−2.55	−0.639
(0,4)	−1.161447 992339 27(6)	35523.359 981 29(1)	−3.12	−0.781
(0,5)	−1.159469 886708 51(8)	35089.215 977 17(2)	−3.81	−0.953
(0,6)	−1.157124 999039 03(9)	34574.572 620 31(2)	−4.61	−1.15
(0,7)	−1.154427 988639 5(1)	33982.647 257 06(2)	−5.53	−1.38
(0,8)	−1.151395 145770 6(1)	33317.015 186 42(2)	−6.54	−1.64
(0,9)	−1.148044 093396 4(1)	32581.544 201 88(2)	−7.64	−1.91
(0,10)	−1.144393 490181 0(1)	31780.329 406 90(2)	−8.82	−2.21
(0,11)	−1.140462 744285 9(1)	30917.630 400 56(2)	−10.1	−2.52
(0,12)	−1.136271 745582 2(2)	29997.812 505 01(3)	−11.3	−2.84
(0,13)	−1.131840 621856 6(3)	29025.293 258 78(7)	−12.7	−3.17
(0,14)	−1.127189 522614 7(3)	28004.494 967 19(7)	−14.0	−3.51
(0,15)	−1.122338 432321 7(3)	26939.803 713 39(7)	−15.4	−3.86
(0,16)	−1.117307 013444 2(3)	25835.534 909 98(7)	−16.8	−4.20
(1,0)	−1.148922 593494 61(3)	32774.352 687 10(1)	−4.54	−1.14
(1,1)	−1.148533 615356 71(3)	32688.981 853 67(1)	−4.68	−1.17
(1,2)	−1.147758 378109 83(3)	32518.836 944 69(1)	−4.95	−1.24
(1,3)	−1.146602 253922 89(4)	32265.097 014 94(1)	−5.35	−1.34
(1,4)	−1.145073 140171 12(4)	31929.495 337 95(1)	−5.88	−1.47
(1,5)	−1.143181 276734 1(1)	31514.279 307 50(2)	−6.52	−1.63
(1,6)	−1.140939 018485 2(1)	31022.160 504 90(3)	−7.27	−1.82
(1,7)	−1.138360 574659 5(2)	30456.257 496 75(4)	−8.13	−2.03
(1,8)	−1.135461 727458 6(1)	29820.034 075 93(2)	−9.07	−2.27
(1,9)	−1.132259 541960 2(3)	29117.235 594 08(7)	−10.1	−2.53
(1,10)	−1.128772 078305 3(3)	28351.825 794 00(7)	−11.2	−2.80
(1,11)	−1.125018 115471 7(4)	27527.926 184 93(9)	−12.3	−3.08
(1,12)	−1.121016 893967 5(2)	26649.759 570 27(5)	−13.5	−3.38
(2,0)	−1.133181 743156 29(4)	29319.635 361 64(1)	−7.11	−1.78
(2,1)	−1.132809 980890 48(6)	29238.042 975 40(2)	−7.23	−1.81
(2,2)	−1.132069 097950 27(6)	29075.437 965 20(2)	−7.49	−1.87
(2,3)	−1.130964 312723 05(8)	28832.965 634 72(2)	−7.86	−1.97
(2,4)	−1.129503 294685 99(8)	28512.309 239 61(1)	−8.35	−2.09
(2,5)	−1.127695 985125 5(2)	28115.650 640 04(5)	−8.95	−2.24
(2,6)	−1.125554 374317 2(2)	27645.621 397 35(5)	−9.65	−2.42
(2,7)	−1.123092 246862 1(2)	27105.246 881 77(5)	−10.4	−2.61
(2,8)	−1.120324 907512 2(2)	26497.886 098 07(5)	−11.3	−2.83
(2,9)	−1.117268 899440 5(2)	25827.169 853 07(5)	−12.3	−3.07
(3,0)	−1.118233 513220 64(5)	26038.878 106 82(2)	−9.39	−2.35

ing dissociation energy $D_{v,J}$ are given in the table. The dissociation energy was obtained from

$$D_{v,j} = 2\mathscr{R}y\left(E(H) + E(D) - E_{v,J}\right), \tag{23}$$

where the nonadiabatic atomic energies $E(H)$ and $E(D)$ are known from the exact solution of the Schrödinger equation. The Rydberg constant $\mathscr{R}y = 109\,737.315\,685\,08(65)\,\mathrm{cm}^{-1}$.[19] All the eigenvalues listed in Table 3 have assigned an uncertainty estimated on the basis of the convergence analysis discussed above. These uncertainties are purely numerical and do not account for those due to physical constants. However, current uncertainties in the proton-electron (deuteron-electron) mass ratio and in the Rydberg constant are more significant than the numerical ones. For example, the CODATA 2014[19] proton-electron and deuteron-electron mass ratios have a relative standard uncertainty of $9.5 \cdot 10^{-11}$ and $3.5 \cdot 10^{-11}$, respectively. A change of this mass ratio by 1σ affects the eigenvalues of HD at the level of 10^{-12} a.u. and the corresponding dissociation energy at $10^{-7}\,\mathrm{cm}^{-1}$. Hence, one cannot exclude the possibility of a refinement of these physical constants in future high-precision studies of HD. Similarly, the current uncertainty in the Rydberg constant affects the conversion of the dissociation energy value from a.u. to reciprocal centimeters at the level of $10^{-7}\,\mathrm{cm}^{-1}$.

Over the decades the fundamental constants were determined with ever increasing accuracy. Not only their uncertainties change but also their estimated values tend to change slightly. This process seems to have accelerated in recent years. For this reason we decided to present the results of our calculations in a form which enables the small changes in the nucleus-to-electron mass ratio to be accounted for. Therefore, apart from the energy evaluated with the CODATA 2014 values of the ratios $\mu_\mathrm{p} = m_\mathrm{p}/m_\mathrm{e}$ and $\mu_\mathrm{d} = m_\mathrm{d}/m_\mathrm{e}$, we supply derivatives of the energy with respect to the change of these ratios $\delta E/\delta\mu_\mathrm{p}$ and $\delta E/\delta\mu_\mathrm{d}$. In case a new recommendation of the proton or deuteron mass appears, the change in μ_p or μ_d can be immediately reflected in the energy of a level by using the derivatives given in Table 3 and the equation

$$E_{v,J}^{\mathrm{new}} = E_{v,J}^{\mathrm{old}} + (\mu_\mathrm{n}^{\mathrm{new}} - \mu_\mathrm{n}^{\mathrm{old}})\frac{\partial E_{v,J}}{\partial \mu_\mathrm{n}}. \tag{24}$$

These derivatives enable also an assessment of the sensitivity of particular levels or pairs of levels to the nuclear mass variations and hence a selection of the best candidates for the future nuclear mass refinement.

The accuracy of the results presented in this work significantly exceeds the accuracy of previously known results. In particular, the best previous dissociation energy of the ground level was obtained from nonadiabatic, explicitly correlated Gaussian functions[14,20] as well as in adiabatic calculations by solving the radial nonadiabatic Schrödinger equation[13]. The comparison presented in Table 4 shows the progress in accuracy made by applying the naJC functions and enables assessment of the accuracy of the other results.

Table 4 Comparison of the best previous literature data with the dissociation energy obtained in this work for the ground level of HD

Year, method, and reference	$D_{0,0}/\mathrm{cm}^{-1}$	Difference
This work	36 406.510 891 37(1)	
2018, 2048-term naECG[20]	36 406.510 879	$1.3 \cdot 10^{-5}$
2010, NAPT[13]	36 406.510 8(10)	$1.1 \cdot 10^{-4}$
2009, 10000-term ECG[14]	36 406.510 46	$4.3 \cdot 10^{-4}$

6 Conclusions

The method described in this work is an extension to the heteronuclear case of the approach presented previously for H_2.[15] As before, bound levels with an arbitrary rotational and vibrational quantum numbers can be accessed. Another extension of the previous approach, crucial from the practical point of view, is the parallelization of the diagonalization procedure. The accuracy achieved for the nonrelativistic energy levels using the nonadiabatic James-Coolidge functions surpasses that obtained with other methods by three or more orders of magnitude. From now the uncertainty of the nonrelativistic component of the total energy no longer limits the overall accuracy. Moreover, thanks to the recent progress in relativistic calculations for HD,[20,21] the uncertainty of the relativistic correction has been significantly diminished (to $2 \cdot 10^{-7}\,\mathrm{cm}^{-1}$) and the current largest contribution to the error budget comes from the missing nonadiabatic quantum electrodynamic effects and amounts to less than $2 \cdot 10^{-4}\,\mathrm{cm}^{-1}$. It is our intention to employ the wave functions obtained within this project to accurately evaluate also the relativistic and QED corrections.

Acknowledgment

The authors wish to acknowledge help from Michał Siłkowski with implementation of the PLASMA library and vectorisation of octuple-precision arithmetics, and from Piotr Kopta with implementation of the Elemental library. This research was supported by the National Science Center (Poland) Grant No. 2017/25/B/ST4/01024, as well as by a computing grant from the Poznan Supercomputing and Networking Center, and by the PRACE project.

References

1 C.-F. Cheng, Y. R. Sun, H. Pan, J. Wang, A.-W. Liu, A. Campargue and S.-M. Hu, *Phys. Rev. A*, 2012, **85**, 024501.
2 D. Mondelain, S. Kassi, T. Sala, D. Romanini, D. Gatti and A. Campargue, *J. Mol. Spectrosc.*, 2016, **326**, 5 – 8.
3 R. K. Altmann, L. S. Dreissen, E. J. Salumbides, W. Ubachs and K. S. E. Eikema, *Phys. Rev. Lett.*, 2018, **120**, 043204.
4 P. Wcisło, F. Thibault, M. Zaborowski, S. Wójtewicz, A. Cygan, G. Kowzan, P. Masłowski, J. Komasa, M. Puchalski, K. Pachucki, R. Ciuryło and D. Lisak, *J. Quant. Spectrosc. Radiat. Transfer*, 2018, **213**, 41 – 51.
5 F. M. J. Cozijn, P. Dupré, E. J. Salumbides, K. S. E. Eikema and W. Ubachs, *Phys. Rev. Lett.*, 2018, **120**, 153002.
6 C. Cheng, J. Hussels, M. Niu, H. L. Bethlem, K. S. E. Eikema, E. J. Salumbides, W. Ubachs, M. Beyer, N. J. Hölsch, J. A.

This journal is © The Royal Society of Chemistry [year]

Agner, F. Merkt, L.-G. Tao, S.-M. Hu and C. Jungen, *Phys. Rev. Lett.*, 2018, **121**, 013001.
7 L.-G. Tao, A.-W. Liu, K. Pachucki, J. Komasa, Y. R. Sun, J. Wang and S.-M. Hu, *Phys. Rev. Lett.*, 2018, **120**, 153001.
8 F. Heiße, F. Köhler-Langes, S. Rau, J. Hou, S. Junck, A. Kracke, A. Mooser, W. Quint, S. Ulmer, G. Werth, K. Blaum and S. Sturm, *Phys. Rev. Lett.*, 2017, **119**, 033001.
9 M. Puchalski, J. Komasa, P. Czachorowski and K. Pachucki, *Phys. Rev. Lett.*, 2016, **117**, 263002.
10 M. Puchalski, J. Komasa and K. Pachucki, *Phys. Rev. A*, 2017, **95**, 052506.
11 W. Kołos and L. Wolniewicz, *Rev. Mod. Phys.*, 1963, **35**, 473.
12 L. Wolniewicz, *J. Chem. Phys.*, 1995, **103**, 1792.
13 K. Pachucki and J. Komasa, *Phys. Chem. Chem. Phys.*, 2010, **12**, 9188.
14 M. Stanke, S. Bubin, M. Molski and L. Adamowicz, *Phys. Rev. A*, 2009, **79**, 032507.
15 K. Pachucki and J. Komasa, *Phys. Chem. Chem. Phys.*, 2018, **20**, 247–255.
16 Y. Hida, X. S. Li and D. H. Bailey, *Quad-Double Arithmetic: Algorithms, Implementation, and Application*, Lbl-46996, lawrence berkeley national laboratory technical report, 2000.
17 J. Poulson, B. Marker, R. A. van de Geijn, J. R. Hammond and N. A. Romero, *ACM Trans. Math. Softw.*, 2013, **39**, 13:1–13:24.
18 A. YarKhan, J. Kurzak, P. Luszczek and J. Dongarra, *Int. J. Parallel Prog.*, 2017, **45**, 612–633.
19 P. J. Mohr, D. B. Newell and B. N. Taylor, *Rev. Mod. Phys.*, 2016, **88**, 035009.
20 M. Puchalski, A. Spyszkiewicz, J. Komasa and K. Pachucki, *Phys. Rev. Lett.*, 2018, **121**, 073001.
21 P. Czachorowski, M. Puchalski, J. Komasa and K. Pachucki, *unpublished*, 2018.